A capacity-enhanced local search for the 5G cell switch-off problem

Francisco Luna[1], Pablo H. Zapata-Cano[1], Ángel Palomares-Caballero[2], Juan F. Valenzuela-Valdés[2]

[1] Department of Computer Science and Programming Languages, University of Málaga. 29071 Málaga, Spain.
{flv,phzc}@lcc.uma.es

[2] Department of Signal Theory, Telematics and Communications – CITIC, University of Granada. 18071 Granada, Spain.
{juanvalenzuela, angelpc}@ugr.es

Abstract. Network densification with deployments of many small base stations (SBSs) is a key enabler technology for the fifth generation (5G) cellular networks, and it is also clearly in conflict with one of the target design requirements of 5G systems: a 90% reduction of the power consumption. In order to address this issue, switching off a number of SBSs in periods of low traffic demand has been standardized as an recognized strategy to save energy. But this poses a challenging NP-complete optimization problem to the system designers, which do also have to provide the users with maxima capacity. This is a multi-objective optimization problem that has been tackled with multi-objective evolutionary algorithms (MOEAs). In particular, a problem-specific search operator with problem-domain information has been devised so as to engineer hybrid MOEAs. It is based on promoting solutions that activate SBSs which may serve users with higher data rates, while also deactivating those not serving any user at all. That is, it tries to improve the two problem objectives simultaneously. The resulting hybrid algorithms have shown to reach better approximations to the Pareto fronts than the canonical algorithms over a set of nine scenarios with increasing diversity in SBSs and users.

Keywords: Problem specific operator · Hybridization · Multi-objective optimization · Cell switch-off problem · 5G networks

1 Introduction

The analysis of the market included in the mobility reports elaborated by Ericcson [7] and Cisco [4] clearly state and confirm the inexorable growth of the mobile subscriptions worldwide, and the consequent increase in the traffic demands, which will not be able to be allocated within the current operative mobile network technologies, mostly the third and fourth generations. With these predictions, both public and private initiatives started to develop the fifth generation (5G) of cellular systems more than a decade ago. The design goals for

such networks to clearly improve upon the existing technologies were quite ambitious [2, 3], aiming, among others, at 1-10Gbps connections, 1 ms latency, 1000x bandwidth, 10-100x connections and, the one that targets this work, 90% of energy consumption to reduce the increasing carbon footprint of this newly 5G networks [18].

Three main paradigms are considered as the key enabler technologies for 5G [14]: use the millimeter wave (mmWave), spectrum, multi-antenna transmission (massive, collaborative MIMO) communications, and network densification. A common fact among them is that they are clearly conflicting the design goal of saving energy. This is specially critical in the third one, which is the target of this work, as 5G networks require the deployment of a large number of small base stations (SBSs), which are close to the mobile users, resulting in the so-called ultra-dense networks (UDN) [9, 12]. Indeed, these dense deployments come with a considerable increase in the power consumption of the system as SBSs are the most consuming device of the network (between 50% to 80%), regardless of its load [19]. In order to address this issue, an already standardized strategy [1] is to switch off a subset of the SBSs in periods of low demand. This is known as the Cell Switch-Off (CSO) problem [8], an NP-complete problem [10] whose search space grows exponentially with the number of SBSs of the UDN. But reducing the energy consumption may be in conflict with maintaining the network operative in terms of the capacity provided to the users, thus clearly driving to a multi-objective optimization problem [11, 15].

The focus of this work is to use multi-objective metaheuristics (MOEAs) [5], more concretely, to enhance the search of two MOEAs, NSGA-II [6] and MOCell [17], by incorporating problem knowledge into their evolutionary loop. We already explored this line of research in [20], where a local search operator that turns off those SBSs that do not have users connected was proposed. This operator was solely aimed at reducing the power consumption of the network, not considering the capacity objective. As a result, the approximated Pareto fronts reached by the hybrid MOEAs clearly explore the regions of the search space that activate the lower number of SBSs, and also provide the User Equipments (UEs) with the lower network capacity. The goal of this work is to introduce a novel local search operator that improves the capacity objective as well. To do so, it works by activating the SBSs that may potentially serve users with higher capacities (i.e., those with larger bandwidth), if the quality of the wireless link, measured in terms of the signal-interference plus noise ratio (SINR), falls below a given threshold. This operator has been called FCSOn, which stands for FemtoCell Switch On, as these are the types of cells of our UDN modeling with the larger operating frequency, and thus the higher available bandwidth. In order to show its effectiveness, it has been incorporated to NSGA-II and MOCell, giving rise to its hybrid versions NSGA-II$_{FCSOn}$ and MOCell$_{FCSOn}$, and they have been compared to both the canonical versions of the algorithms and the previous devised operator [20] on a set of 9 different scenarios with increasing densification. The results have shown that the search of these two new hybrid MOEAs are capable of better reaching non-dominated solutions with higher capacity.

Table 1: Model parameters for BSs and UEs

Cell	Parameter	LL	LM	LH	ML	MM	MH	HL	HM	HH
macro	G_{tx}	14								
	f	2 GHz (BW = 100 MHz)								
micro1	G_{tx}	12								
	f	3.5 GHz (BW = 175 MHz)								
	λ_P^{micro1} $[BS/km^2]$	100	100	100	200	200	200	300	300	300
micro2	G_{tx}	10								
	f	5 GHz (BW = 250 MHz)								
	λ_P^{micro2} $[BS/km^2]$	100	100	100	200	200	200	300	300	300
pico1	G_{tx}	5								
	f	10 GHz (BW = 500 MHz)								
	λ_P^{pico1} $[BS/km^2]$	500	500	500	600	600	600	700	700	700
pico2	G_{tx}	7								
	f	14 GHz (BW = 700 MHz)								
	λ_P^{pico2} $[BS/km^2]$	500	500	500	600	600	600	700	700	700
femto1	G_{tx}	4								
	f	28 GHz (BW = 1400 MHz)								
	λ_P^{femto1} $[BS/km^2]$	1000	1000	1000	2000	2000	2000	3000	3000	3000
femto2	G_{tx}	3								
	f	66 GHz (BW = 3300 MHz)								
	λ_P^{femto2} $[BS/km^2]$	1000	1000	1000	2000	2000	2000	3000	3000	3000
UEs	λ_P^{UE} $[UE/km^2]$	1000	2000	3000	1000	2000	3000	1000	2000	3000

The work has been structured as follows. The next section formally describes the model of the UDN used, as well as the formulation of the problem objectives for both the CSO problem. Section 3 details the FSOn operator and its integration in NSGA-II and MOCell. The experimental methodology and the analysis of the results is carried out in the Sect. 4. Finally, the main conclusions of the work as well as the lines for future research are included in Sect. 5.

2 Problem modeling

This section first introduces the modeling of the UDN and, then, a mathematical formulation of the CSO problem is provided.

2.1 UDN modeling

This work considers a service area of 500×500 square meters, which has been discretized using a grid of 100×100 points (also called "pixels" or area elements), each covering a 25 m^2 area, where the signal power is assumed to be constant. Ten different regions have been defined with different propagation conditions. In order to compute the received power at each point, $P_{rx}[dBm]$, the following model has been used:

$$P_{rx}[dBm] = P_{tx}[dBm] + PLoss[dB] \quad (1)$$

where, P_{rx} is the received power in dBm, P_{tx} is the transmitted power in dBm, and $PLoss$ are the global signal losses, which depend on the given propagation region, and are computed as:

$$PLoss[dB] = GA + PA \tag{2}$$

where GA is the total gain of both antennas, and PA are the transmission losses in space, computed as:

$$PA[dB] = \left(\frac{\lambda}{2 \cdot \pi \cdot d}\right)^K \tag{3}$$

where d is the Euclidean distance to the SBS, K is the exponent loss, which ranges randomly in $[2.0, 4.0]$ for each of the 10 different regions. The signal to interference plus noise ratio (SINR) for User Equipment (UE) k, is:

$$SINR_k = \frac{P_{rx,j,k}[mW]}{\sum_{i=1}^{M} P_{rx,i,k}[mW] - P_{rx,j,k}[mW] + P_n[mW]} \tag{4}$$

where $P_{rx,j,k}$ is the received power by UE k from SBS j, the summation is the total received power by UE k from all the SBSs operating at the same frequency that j, and P_n is the noise power, computed as:

$$P_n[dBm] = -174 + 10 \cdot \log_{10} BW_j \tag{5}$$

being BW_j the bandwidth of SBS j, defined as the 5% of the SBS operating frequency (see Table 1). Finally, the capacity of the UE k is:

$$C_k^j[bps] = BW_k^j[Hz] \cdot \log_2(1 + SINR_k) \tag{6}$$

where BW_k^j corresponds to the bandwidth assigned to the UE k when connected to the SBS j, assuming a round robin scheduling, that is:

$$BW_k^j = \frac{BW_j}{N_j} \tag{7}$$

where N_j is the number of UEs connected to SBS j, assuming that UEs are connected to the SBS with the highest SINR, regardless of its type.

Four different types of cells of decreasing size are considered (fully heterogeneous network): femtocells, picocells, microcells, and macrocells. Two subtypes of femto, pico, and microcells are also defined, summing up 7 cell types (see Table 1). The SBSs that serve these cells all have a transmitting power of $P_{tx} = 750mW$, so their actual coverage is defined by their operating frequencies and the consequent losses that considers the SINR (the higher the frequency, the lower the coverage). Also, SBSs are deployed using an independent Poisson Process (PPP) with different densities (defined by λ_P^{BS}). UEs are also positioned using a PPP with a value of λ_P^{UE}, but using social attractors (SAs), following the procedure proposed in [16]. This deployment scheme also uses two factors α and μ_β, which indicate how strong the attraction of BSs to SAs is (same applies for SAs to UEs). The values used in the simulations are $\alpha = \mu_\beta = 0.25$.

The detailed parametrization of the addressed scenarios is included in Table 1, in which the names in the last nine columns, XY, stand for the deployment densities of SBSs and UEs, respectively, so that X = {L, M, H}, meaning either low, medium, or high density deployments (λ_P^{SBS} parameter of the PPP), and Y = {L, M, H}, indicates a low, medium or high density of deployed UEs (λ_P^{UE} parameter of the PPP). The parameters G_{tx} and f of each type of cell refer to the transmission gain and the operating frequency (and its available bandwidth) of the antenna, respectively.

2.2 The CSO problem

Let $\mathcal{B}$ be the set of the SBSs randomly deployed. A solution to the CSO problem is a binary string $s \in \{0,1\}^{|\mathcal{B}|}$, where s_i indicates whether SBS i is activated or not. The first objective to be minimized is therefore computed as:

$$\min f_{Power}(s) = \sum_{i=1}^{|\mathcal{B}|} s_i \tag{8}$$

that is, the number of active SBSs in the network.

Let $\mathcal{U}$ be the set of the UEs also deployed as described in the section above. In order to compute the total capacity of the system, UEs are first assigned to the active SBS that provides the highest SINR. Let $\mathcal{A}(s) \in \{0,1\}^{|\mathcal{U}|\times|\mathcal{B}|}$ be the matrix where $a_{ij} = 1$ if $s_j = 1$ and SBS j serves UE i with the highest SINR, and $a_{ij} = 0$ otherwise. Then, the second objective to be maximized, which is the total capacity provided to all the UEs, is calculated as:

$$\max f_{Cap}(s) = \sum_{i=1}^{|\mathcal{U}|} \sum_{j=1}^{|\mathcal{B}|} s_j \cdot a_{ij} \cdot BW_i^j \tag{9}$$

where BW_i^j is the shared bandwidth of SBS j provided to UE i (Eq. 7). We would like to remark that these two problem objectives are clearly in conflict with each other, as switching off base stations, that is, minimizing the power consumption of the network, will clearly decrease its capacity because the available bandwidth to serve users is reduced.

3 Hybrid MOEAs: The FCSOn Operator

This section details, firstly, the solution representation used to address the CSO and the genetic operators of the two MOEAs. Secondly, a description of the FCSOn operator is provided, followed by the contributions of this work. Finally, a brief description of NSGA-II and MOCell and how they integrate the operator within its evolutionary cycle is given.

3.1 Representation and genetic operators

The representation used for the candidate solutions is the canonical binary string, in which each gene corresponds to a SBS, and indicates whether it is on ('1') or off ('0'). The selection, crossover and mutation operators are, respectively, binary tournament, two-point crossover with $r_c = 0.9$, and flip bit mutation with $r_m = 1/L$, where L is the number of SBSs of the UDN. The stopping condition is to reach 100000 evaluations of the objective functions. All the algorithms used in this work have been implemented in the jMetal framework[3].

3.2 The FCSOn operator

As stated in the introduction section, this is a capacity-based operator as it aims at increasing the capacity the UDN provides to the UEs by switching on femtocells that may act as serving cells. Recall that this type of cells are those with the higher available bandwidth (they have the higher operating frequency)

[3] `https://github.com/jMetal/`

when users are rather close to them. We assume this closeness to be enough when the SINR received by the UE u from the a femtocell f is greater than 1 dB. If this holds, then the f is switched on as is could be a potential candidate to serve u with higher capacity. If the current cell that serves u has no more users connected, then it is switched off. The FCSOn operator builds upon the CSO operator presented in [20], which deactivates those cells not having any UE connected. Whereas the CSO operator clearly targets only the power consumption objective, the FCSOn operator also aims at improving the capacity. Algorithm 1 sketches the pseudocode of the operator.

3.3 Hybrid algorithms NSGA-II$_{FCSOn}$ y MOCell$_{FCSOn}$

This section first outlines the template of a generic MOEA (Algorithm 2), to further describe the canonical versions of NSGA-II and MOCell afterwards. Then, based upon this template, the modifications required to include the FCSOn operator are detailed.

The NSGA-II algorithm (*Non-dominated Sorting Genetic Algorithm II*) [6] is a genetic algorithm that works by generating, from a population P_t, another auxiliary population Q_t using the genetic operators of selection, crossover and mutation (line 8 of the Algorithm 2); then, the solutions included in $P_t \cup Q_t$ are ordered according to their rank and, those with the best (lowest) values of this quality indicator, are passed on to the next generation P_{t+1} (line 11). For selecting among solutions with the same range, NSGA-II uses a density estimator that promotes solutions from the less populated areas of the approximated front.

MOCell (Multi-Objective Cellular Genetic Algorithm) is a cellular genetic algorithm [17] that includes an external file to store the non-dominated solutions found during the search (line 4 in Algorithm 2). This archive is bounded and uses the same density estimator of NSGA-II to maintain the diversity of solutions along the approximated Pareto front. Its major contributions lies in the neighborhood relationship between solutions, as the population is structured in a 2D toroidal mesh, defining a set of neigboring solutions that is used in the evolutionary cycle.

Algorithm 1 Pseudocode of the FCSOn operator

```
1: U ← GetUsersNotServedByFemtoCell()
2: for u in U do
3:    current ← GetServingCell(u)
4:    C ← GetFemtoCellsWithHigherSINR(u)
5:    for c in C do
6:       if SINR(u,c) > 1 dB then
7:          Activate(c)
8:          SetServingCell(u,c)
9:       end if
10:   end for
11: end for
12: ApplyCSOOperator() //see [20] for the details
```

Algorithm 2 Template of a multi-objective metaheuristics

```
1: S(0) ← GenerateInitialPopulation()
2: A(0) ← ∅
3: Evaluate(S)
4: A(0) ← Update(A(0), S(0))
5: t ← 0
6: while not StoppingCondition( ) do
7:    t ← t + 1
8:    S(t) ← GeneticOperators(A(t − 1), S(t − 1))
9:    Evaluate(S′(t))
10:   A(t) ← Update(A(t), S′(t))
11: end while
12: Output: A
```

Algorithm 3 NSGA-II$_{FCSOn}$ and MOCell$_{FCSOn}$

```
8: S(t) ← GeneticOperators(A(t − 1), S(t − 1))
9: r ← Random(0, 1)
10: if r < r_FCSOn then
11:    S′(t) ← FCSOn(S(t))
12: end if
13: Evaluate(S′(t))
14: A(t) ← Update(A(t), S′(t))
```

The FCSOn operator has been integrated within the NSGA-II and MOCell evolutionary cycle by replacing Algorithm 2 lines 8 to 10 with those of the Algorithm 3. Right after applying genetic operators, and before evaluating to determine whether or not to incorporate them into the next generation of algorithm solutions, the local search is applied with a given rate, r_{FCSOn}.

4 Experimentation

This section describes the methodology used to conduct the experiments, showing the effectiveness of the new hybrid proposals, NSGA-II$_{FCSOn}$ and MOCell$_{FCSOn}$, as well as the analysis of the obtained results.

4.1 Methodology

Since metaheuristics are stochastic algorithms, 30 independent runs of each algorithm for each of the nine scenarios have been performed. Each run addresses a random instance of the problem, but the same 30 seeds are used to ensure that all algorithms tackle the same set of instances. Two indicators have been used to measure the quality of the approaches to the Pareto front achieved by the four algorithms: the hypervolume (HV) [21] and the attainment surfaces [13].

The HV is considered as one of the more suitable indicators in the multi-objective community. Higher values of this metric are better. Since this indicator is not free from an arbitrary scaling of the objectives, we have built up a reference Pareto front (RPF) for each problem composed of all the nondominated solutions

found for each problem instance by all the algorithms. Then, the RPF is used to normalize each approximation prior to compute the HV value. While the HV allows one to numerically compare different algorithms, from the point of view of a decision maker, it gives no information about the shape of the front. The empirical attainment function (EAF) [13] has been defined to do so. EAF graphically displays the expected performance and its variability over multiple runs of a multi-objective algorithm.

4.2 Results of the HV indicator

This section first starts by analyzing the effect of the hybridization of NSGA-II and MOCell with the FCSOn operator in the HV indicator. To do so, taking the base setting for the two algorithms described in Sect. 3.1, two different values for r_{FCSOn} have been evaluated: 0.01 and 0.1, the same as in our previous work [20]. This value is superscripted to NSGA-II$_{FCSOn}$ and MOCell$_{FCSOn}$ for a better identification in Table 2, which includes the average HV values and its standard deviation for both the canonical algorithms and their hybrid versions. A grey coloured background has been used to highlight the best (highest) value for each algorithm.

The first clear conclusion drawn from the results is that the hybrid algorithms are always reaching approximated fronts with higher (better) HV values (no row for the NSGA-II and MOCell columns are highlighted). This means that the problem-domain information included in the algorithms has improved the search performance. The second conclusion is that, as long as the scenarios gain in density, the gap between the HV value of the canonical algorithm and the hybrid versions increases, thus resulting to approximated Pareto fronts with lower power consumption and higher capacity. Indeed, averaging over all the LX, MX, and HX scenarios results in a HV gap of 0.02, 0.09 and 0.16, respectively. Figure 1 displays the statistical analysis of the results. It shows that differences become statistically significant with the size of the instances gets larger.

Table 2: HV results for all algorithms over the 9 scenarios

	NSGA-II	NSGA-II$^{0.01}_{FCSOn}$	NSGA-II$^{0.1}_{FCSOn}$	MOCell	MOCell$^{0.01}_{FCSOn}$	MOCell$^{0.1}_{FCSOn}$
LL	0.3327 ±0.0766	0.3678 ±0.1041	0.3653 ±0.0990	0.3413 ±0.0849	0.3553 ±0.0852	0.3663 ±0.1008
LM	0.3702 ±0.1064	0.4081 ±0.1171	0.4084 ±0.1218	0.3596 ±0.1015	0.3848 ±0.1100	0.3945 ±0.1137
LH	0.4229 ±0.1463	0.4642 ±0.1496	0.4483 ±0.1534	0.4032 ±0.1305	0.4263 ±0.1457	0.4349 ±0.1304
ML	0.2541 ±0.0635	0.3345 ±0.1008	0.3349 ±0.0989	0.2677 ±0.0698	0.3086 ±0.0789	0.3223 ±0.0909
MM	0.1827 ±0.0949	0.3243 ±0.1507	0.3211 ±0.1414	0.1747 ±0.0934	0.2920 ±0.1344	0.2953 ±0.1368
MH	0.2729 ±0.1156	0.3721 ±0.1633	0.3705 ±0.1664	0.2661 ±0.1147	0.3411 ±0.1500	0.3438 ±0.1487
HL	0.1527 ±0.0616	0.3690 ±0.0950	0.3857 ±0.0921	0.2497 ±0.0663	0.3653 ±0.0867	0.3715 ±0.0922
HM	0.0968 ±0.0676	0.3357 ±0.1129	0.3536 ±0.1088	0.1930 ±0.0795	0.3315 ±0.1025	0.3315 ±0.1041
HH	0.1349 ±0.0642	0.3302 ±0.1219	0.3329 ±0.1210	0.2116 ±0.0800	0.3278 ±0.1089	0.3203 ±0.1022

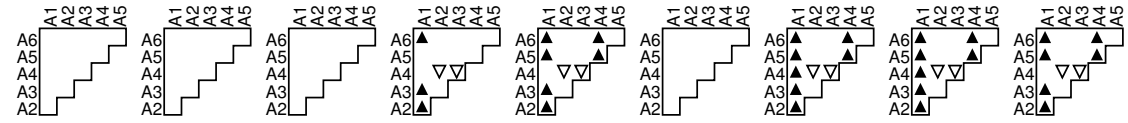

(a) LL (b) LM (c) LH (d) ML (e) MM (f) MH (g) HL (h) HM (i) HH

Legend: A1 = NSGA-II, A2 = NSGA-II$^{0.01}_{FCSOn}$, A3 = NSGA-II$^{0.1}_{FCSOn}$
A4 = MOCell, A5 = MOCell$^{0.01}_{FCSOn}$, A6 = MOCell$^{0.1}_{FCSOn}$

Fig. 1: Statistical analysis of the HV results for each of the 9 scenarios.

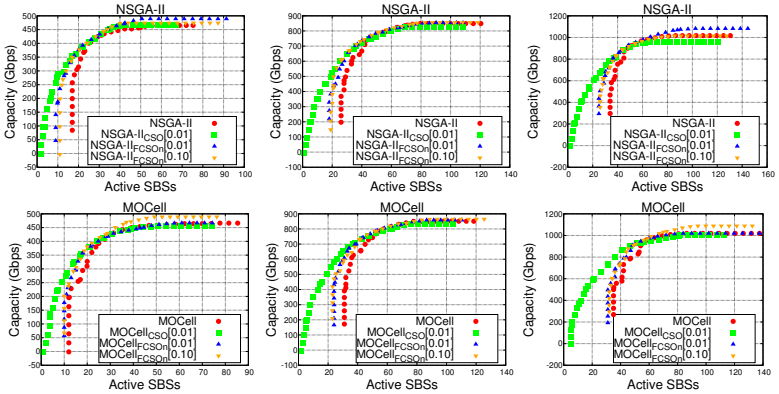

(a) LL scenario (b) LM scenario (c) LH scenario

Fig. 2: Attainment surfaces of NSGA-II and NSGA-II$_{FCSOn}$ (top), and MOCell and MOCell$_{FCSon}$ (bottom), for the three scenarios with a lower SBS density.

As to the effect of the application rate of the FCSOn operator, r_{FCSOn}, it can be observed that, in general (12 out of the 18 cases), the setting with 0.1 has obtained higher HV values. This is a very promising finding, as it opens a research line to further enhance the search capabilities of the MOEAs for this problem by promoting the use of the smallest SBSs of the network, which are not only the more numerous, but also the ones that provide the higher bandwidth. They are those that also consume the lower power consumption.

Finally, and as it consistently occurred with the search operator devised in our previous paper, it can also be seen that NSGA-II has better integrated the newly generated genetic material within the search than MOCell, because in the initial study on this problem [15], NSGA-II was outperformed by MOCell, and now the situation with the hybrid version has been reversed, that is, NSGA-II$_{FCSOn}$ has always obtained a higher HV value (except for the LL instance).

4.3 Attainment surfaces

In order to graphically show the actual differences of the approximated Pareto fronts reached by the hybrid algorithms that uses the FCSOn operator, Figs. 2, 3, and 4 includes the 50%-attainment surfaces of the algorithms for the LX, MX and HX scenarios, respectively. The figures have been arranged in two rows, with the surfaces of NSGA-II at the top, and those of MOCell at the bottom.

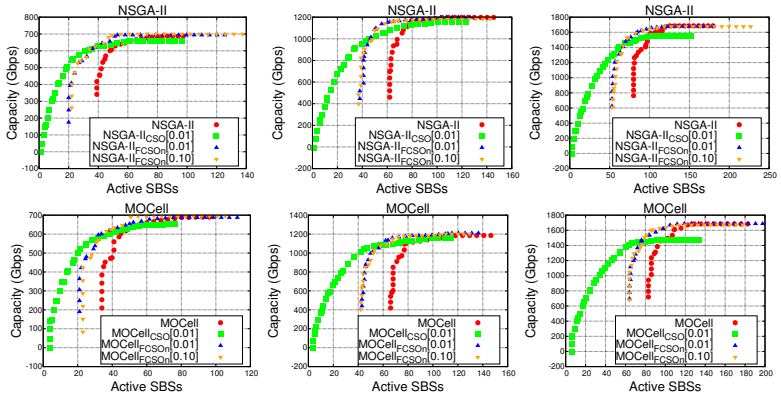

(a) ML scenario (b) MM scenario (c) MH scenario

Fig. 3: Attaiment surfaces of NSGA-II and NSGA-II$_{FCSOn}$ (top), and MOCell and MOCell$_{FCSon}$ (bottom), for the three scenarios with a medium SBS density.

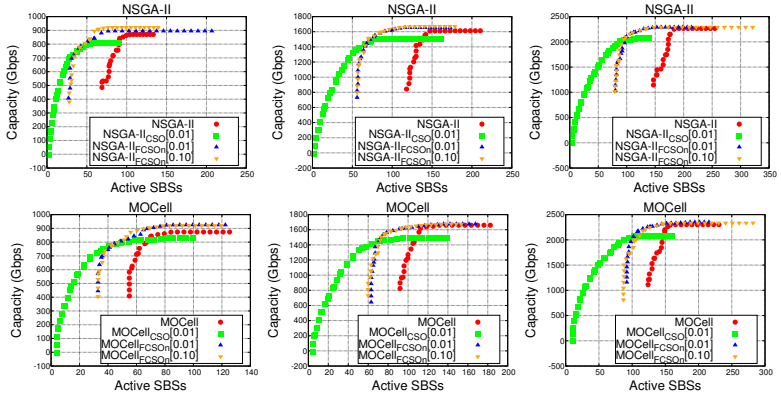

(a) HL scenario (b) HM scenario (c) HH scenario

Fig. 4: Attaiment surfaces of NSGA-II and NSGA-II$_{FCSOn}$ (top), and MOCell and MOCell$_{FCSon}$ (bottom), for the three scenarios with a high SBS density.

The figures not only display the attainment surfaces of the canonical algorithms and the FCSOn-based hybrid versions of the algorithms, but also that of the CSO operator obtained in [20].

A first common, clear fact in all figures is that the CSO-based hybrid has always explored better the region of the search space with a smaller number of active SBSs (lower consumption), that is, the left-hand side of the displayed graphics. But this is expected, because the CSO operator has been devised only targeting this problem objective (recall, it is based on switching off SBSs not serving any UE). The second conclusion is that the median approximated fronts of the FCSOn-based hybrids always dominate those of the canonical algorithms, and improving upon the two objectives (not only in the power consumption, as the CSO-base one does), thus also reaching solutions with higher capacity. This is specially relevant in the LL, LH, and HL scenarios.

This visual inspection of the median approximated fronts clearly shows that the initial working hypothesis of developing an capacity-based operator that also accounts for the capacity objective has been achieved. Our goal of promoting the activation of close, high bandwidth femtocells has enabled the hybrid algorithms to explore a complex region of the search space. It is complex because increasing the capacity is not an easy task as it requires to minimize interferences (to increase the SINR), which is done by deactivating SBSs. That is, the FCSOn operator has reached a proper balance between activation and deactivation of SBSs. Indeed, we would also like to remark the newly proposed FCSOn operator has been able to improve the energy consumption objective, activating an smaller number of SBSs than the canonical algorithms do.

5 Conclusions

This work has addressed the Cell-Switch Off problem in ultra-dense network deployments required for the fifth generation of telecommunication systems. It has been formulated as a multi-objective optimization problem with two conflicting objectives: minimizing the power consumption measured in terms of the number of active base stations, and maximizing the capacity provided to the end users (GBps in downlink). In this context, a new capacity-enhanced local search operator aiming at promoting the association of users to femtocells, called FCSOn, is devised. The rational behind this problem-specific knowledge is that this type of cells are those that provide the higher bandwidth (higher capacity). The FCSOon operator is built upon a previous operator that also deactivates all the cells with no users assigned, thus also targeting a reduction of the power consumption. The integration within NSGA-II and MOCell has resulted in an enhanced exploration of the search space that has reached solutions that improve the two problem objectives. It has been shown both numerically, by using the HV indicator and, graphically and more clearly, with the attainment surfaces. As future work we plan to better characterize this operator, measuring the impact of the threshold it requires (set to 1 dB), and also to devise other operators that keep improving the search of multi-objective metaheuristics. Evaluating the impact of the operator in other MOEAs will also be considered.

Acknowledgements

This work has been supported by the the Spanish and Andalusian goverments, and FEDER, under contrats TIN2016-75097-P, RTI2018-102002-A-I00 and B-TIC-402-UGR18. Francisco Luna also acknowledges support from Universidad de Málaga. The authors thankfully acknowledges the support provided by the Supercomputing and Bioinformatics center of the University of Málaga.

References

1. 3GPP: Small Cell Enhancements for E-UTRA and E-UTRANPhysical Layer Aspects. Tech. rep., 3rd Generation Partnership Project (3GPP) (2014), http://www.3gpp.org/ ftp/Specs/html-info/36872.htm

2. Andrews, J.G., Buzzi, S., Choi, W., Hanly, S.V., Lozano, A., Soong, A.C.K., Zhang, J.C.: What Will 5G Be? IEEE J. on Sel. Areas in Comm. **32**(6), 1065–1082 (2014)
3. Bohli, A., Bouallegue, R.: How to meet increased capacities by future green 5g networks: A survey. IEEE Access **7**, 42220–42237 (2019)
4. Cisco: Global mobile data traffic forecast update, 20172022 white paper. https://www.cisco.com/c/en/us/solutions/collateral/service-provider/visual-networking-index-vni/white-paper-c11-738429.html (2019), accessed June 8, 2019
5. Coello Coello, C.A., Lamont, G.B., Van Veldhuizen, D.A.: Evolutionary Algorithms for Solving Multi-Objective Problems. Springer, New York (2007)
6. Deb, K., Pratap, A., Agarwal, S., Meyarivan, T.: A fast and elitist multiobjective genetic algorithm: NSGA-II. IEEE Trans. on Ev. Comp. **6**(2), 182 – 197 (2002)
7. Ericsson: Ericsson mobility report. https://www.ericsson.com/en/mobility-report/reports/q4-update-2018 (2018), accessed June 8, 2019
8. Feng, M., Mao, S., Jiang, T.: Base station on-off switching in 5g wireless networks: Approaches and challenges. IEEE Wireless Communications **24**(4), 46–54 (2017)
9. Ge, X., Tu, S., Mao, G., Wang, C.X., Han, T.: 5G Ultra-Dense Cellular Networks. IEEE Wireless Communications **23**(1), 72–79 (feb 2016)
10. Gonzalez, D., et al.: A Novel Multiobjective Cell Switch-Off Framework for Cellular Networks. IEEE Access **4**, 7883–7898 (2016)
11. González, D., Mutafungwa, E., Haile, B., Hämäläinen, J., Poveda, H.: A Planning and Optimization Framework for Ultra Dense Cellular Deployments. Mobile Information Systems **2017**, 1–17 (2017)
12. Kamel, M., Hamouda, W., Youssef, A.: Ultra-Dense Networks: A Survey. IEEE Communications Surveys & Tutorials **18**(4), 2522–2545 (2016)
13. Knowles, J.: A summary-attainment-surface plotting method for visualizing the performance of stochastic multiobjective optimizers. In: 5th International Conference on Intelligent Systems Design and Applications. pp. 552 – 557 (2005)
14. Lopez-Perez, D., Ding, M., Claussen, H., Jafari, A.H.: Towards 1 Gbps/UE in Cellular Systems: Understanding Ultra-Dense Small Cell Deployments. IEEE Communications Surveys & Tutorials **17**(4), 2078–2101 (2015)
15. Luna, F., Luque-Baena, R., Martínez, J., Valenzuela-Valdés, J., Padilla, P.: Addressing the 5g cell switch-off problem with a multi-objective cellular genetic algorithm. In: IEEE 5G World Forum, 5GWF 2018. pp. 422–426 (2018)
16. Mirahsan, M., Schoenen, R., Yanikomeroglu, H.: HetHetNets: Heterogeneous Traffic Distribution in Heterogeneous Wireless Cellular Networks. IEEE Journal on Selected Areas in Communications **33**(10), 2252–2265 (2015)
17. Nebro, A.J., Durillo, J.J., Luna, F., Dorronsoro, B., Alba, E.: Mocell: A cellular genetic algorithm for multiobjective optimization. Int. J. of Intelligent Systems **24**(7), 723 – 725 (2009)
18. Piovesan, N., Fernandez Gambin, A., Miozzo, M., Rossi, M., Dini, P.: Energy sustainable paradigms and methods for future mobile networks: A survey. Computer Communications **119**(December 2017), 101–117 (2018)
19. Yao, M., Sohul, M.M., Ma, X., Marojevic, V., Reed, J.H.: Sustainable green networking: exploiting degrees of freedom towards energy-efficient 5G systems. Wireless Networks **25**(3), 951–960 (apr 2019)
20. Zapata-Cano, P., Luna, F., Valenzuela-Valdés, J., Mora, A.M., Padilla, P.: Metaheurísticas híbridas para el problema del apagado de celdas en redes 5G (in Spanish). In: MAEB'18. pp. 665 – 670 (2018)
21. Zitzler, E., Thiele, L.: Multiobjective evolutionary algorithms: a comparative case study and the strength pareto approach. IEEE Trans. Evolutionary Computation **3**(4), 257–271 (1999)